

Assessment of Iron Stores in Children With Transfusion Siderosis by Biomagnetic Liver Susceptometry

Roland Fischer,^{1*} Christian D. Tiemann,² Rainer Engelhardt,¹ Peter Nielsen,¹ Matthias Dürken,² Erich E. Gabbe,¹ and Gritta E. Janka²

¹Abteilung Medizinische Biochemie, University Hospital Eppendorf, Hamburg, Germany

²Abteilung Pädiatrische Hämatologie und Onkologie, University Hospital Eppendorf, Hamburg, Germany

To investigate the applicability of noninvasive Superconducting Quantum Interference Device (SQUID) biomagnetic liver susceptometry and its limitations in thalassemic children, 23 patients with β -thalassemia major and other iron loading anemias (age: 4–16 years) and 16 age-related normal children were studied. Liver iron concentrations ranged from 600 to 11,000 $\mu\text{g/g}_{\text{liver}}$ for thalassemic patients and from 60 to 340 $\mu\text{g/g}_{\text{liver}}$ for normal patients. Measuring the respective organ volumes by sonography, liver and spleen iron stores, accounting for 80% of total body iron stores, were estimated. Nonliver contributions from the lung or intestine to the measured SQUID signals in the small-sized patients were not observed. Moreover, livers in thalassemia were found to be enlarged by 18% per 1,000 $\mu\text{g/g}$ ($r = 0.75$, $P < 10^{-3}$). Serum ferritin values correlate significantly with iron stores ($r = 0.64$, $P < 10^{-3}$), but predict iron stores only within large error intervals of 4,000 $\mu\text{g/g}_{\text{liver}}$. Analyzing the experimental data from biomagnetometry and from related transfusion and chelation treatment data within the framework of a two-compartment model, we were able to derive additional information on total body iron elimination and chelation therapy efficacy. The exponential decline of iron stores allows forecast of steady-state conditions of the final iron load for a particular transfusion and chelation therapy regimen. *Am. J. Hematol.* 60:289–299, 1999. © 1999 Wiley-Liss, Inc.

Key words: iron; children; thalassemia; chelation therapy; SQUID; biomagnetometry

INTRODUCTION

Patients with iron loading anemias such as thalassemia need regular blood transfusions. The consequence of this therapy is an increased iron accumulation in a variety of organs, especially the liver. Due to the increased iron stores, first in the macrophages of the reticuloendothelial system and then after redistribution into the parenchymal cells, these patients are at high risk for iron-induced cardiomyopathy, diabetes, and hepatic cirrhosis [1]. To protect thalassemic patients, especially children, against these risk factors, it is crucial that the iron accumulation is kept at reasonably low values by a certain iron chelation therapy regimen. On the other hand, drug toxicity from overdosing of chelation therapy has to be avoided. Several invasive and noninvasive methods now exist for monitoring iron overload with different degrees of precision and reliability [2]. Noninvasive biomagnetic liver susceptometry (BLS) offers the possibility to monitor routinely iron overload during chelation therapy with sufficient precision in young and adult patients [3,4].

Nevertheless, acceptance of this method by clinical centres is limited by its apparent complexity and availability at only two centres in the world (Cleveland and Hamburg). However, this situation may change now with new efforts to enhance clinicians' awareness of this method [5].

Because biosusceptometry, in contrast to quantitative magnetic resonance imaging, has only a limited spatial resolution, current detector configurations may not be suited for the smaller-sized livers and bodies in children. Moreover, there were concerns about the practicability of this method in young children because of the use of a

C.D. Tiemann is now at Kinderklinik, University of Freiburg.

*Correspondence to: Dr. Roland Fischer, Abt. Medizinische Biochemie, UKE–Inst. f. Physiol.–Chemie, D-20246 Hamburg, Germany. E-mail: fischer@uke.uni-hamburg.de

Received for publication 9 April 1998; Accepted 2 December 1998

water interface of 6–8 kg [6]. This study aimed to investigate the applicability of Superconducting Quantum Interference Device (SQUID) biomagnetometry and its limitations in thalassemic children. The additional investigation of normal age-matched children would also reveal any shortcomings with respect to sensitivity, precision, spatial resolution, and patient noise from nonliver contributions. The measurement of liver iron concentration (LIC) is only a first step in the assessment of total body iron stores and at least, must be related to liver size [7, p 215], especially as livers (and spleens) are often enlarged in thalassemic patients.

Besides the well-established chelation therapy with deferoxamine (DFO), the oral chelator deferiprone (L1) is available at least for compassionate use. To evaluate the efficacy of these and forthcoming novel chelators, iron balance kinetics have to be described in a quantitative manner in relation to the iron influx from red cell transfusions, the chelator and its dosage, the change in total body iron stores, and the iron efflux by urinary and fecal excretion [8]. The analysis of biomagnetometry derived parameters in the framework of a mathematical model produces a more complete picture of thalassemia than could be derived from measurement of LIC alone.

MATERIALS AND METHODS

Patients and Normal Subjects

In 23 patients (aged 2–31 years) with β -thalassemia major (14) or intermedia (4), and other iron loading anemias (5), liver and spleen iron concentrations were determined from biomagnetic susceptibility measurements and compared with results from 16 normal children and young adults (aged 7–25 years). The patients were investigated during their routine checkup before blood transfusion in the hospital and informed consent was given by all subjects or parents. All thalassemic patients had been transfusion dependent since early childhood and on regular chelation therapy regimen with s.c. DFO since the age of 4 to 7 years. In five patients biomagnetometry could be performed before the onset of the first regular chelation therapy. These patients had received only single doses of DFO (3 g) at the time of transfusion of filtered erythrocyte concentrates.

Clinical Parameters

The net weight of filtered erythrocyte concentrates (EC) was documented during each transfusion. The amount of iron from one EC was calculated from the data of the hospital's blood bank (243 ± 19 ml/EC with 0.245 ± 0.007 g Hb/ml).

All patients were tested regularly for standard biochemical parameters, especially for serum levels of the liver enzyme alanine aminotransferase (ALT) and for antibodies of a hepatitis C virus infection (HCV). Only

four of the 23 patients tested positively for HCV infection. Serum ferritin concentration was measured in our laboratory by an immunoradiometric assay (Ramco Lab., Houston, TX) adjusted by the international ferritin standard WHO 80/602. At least three ferritin values within two transfusion intervals nearest to the BLS measurement were averaged, excluding increased values by elevated ALT levels.

SQUID Biosusceptometry

The biomagnetic measurements were performed by lowering the patient in the constant nonuniform magnetic field of the Hamburg Biosusceptometer (Ferritometer®, BTi, San Diego, CA), with a water coupling membrane as a reference medium [3] instead of the air reference favored by Hartmann et al. [6]. The system, with two 2nd order gradiometers and rf-SQUIDS for magnetic flux amplification, has been described in more detail elsewhere [9]. In short, bed-side sonography (positioning, liver/spleen contour, and volume estimation) was done on patients in the supine position by laser-cross alignment. Patients with the water coupling membrane above the liver or spleen (water pressure: 6–9 kg) were lowered dynamically by 7 cm at a maximum speed of 0.7 cm/sec within the magnetic field of the superconducting coils. Patients stopped breathing for 10 sec during the measurement, in most cases in an exhaled state. The breathing of very young children did not result in serious noise contributions from lung tissue. However, to stabilize a found optimum position could become more difficult. Therefore, in young patients (<5 years) a sedation may be envisaged.

On average, three measurement runs vs. the water reference medium and one vs. the air reference were obtained. Data analysis of the registered SQUID voltages was done by modeling of the magnetic flux change from ellipsoidal organ and cylindrical/hemispherical body geometries as a function of the liver-skin-detector distance [10]. The concentrations of paramagnetic human hemosiderin/ferritin iron in liver and spleen were calculated from the magnetic organ susceptibilities by means of the specific magnetic susceptibility of human ferritin iron [11]. The calibration of this method was performed by the physical measurement of an infinite water half space, resulting in an adjustment of the calibration factor to an equivalent ferritin iron concentration of $5,873 \mu\text{g/ml}$. This avoided any uncertainties in geometry and magnetic susceptibility. A verification of LIC from BLS has been accomplished previously by liver biopsies from patients with genetic hemochromatosis [4,10]. A homogeneous susceptibility, i.e., a homogeneous liver iron distribution, was assumed in the detection region of interest (diameter: 7 cm; depth: 3.5 cm). At optimum measuring positions in adults, the interfering effects from surrounding paramagnetic tissues (lungs, intestine) and deep-lying

large blood vessels could be neglected due to the localized magnetic sensitivity.

Although the system sensitivity was equivalent to 20 $\mu\text{g/g}_{\text{liver}}$ [9], larger overall errors had to be expected in patient measurements with this nonlocalizing method. Besides the statistical error of about 20 to 100 $\mu\text{g Fe/g}_{\text{liver}}$ from three to four measurement runs, systematic errors in the skin–liver distance of $\Delta z_{\text{liver}} = 0.5 \text{ mm}$ and in the thorax tissue susceptibility of $\Delta \chi_{\text{tissue}} = 0.05 \cdot 10^{-6} \text{ SI units}$ were assumed. The influence of these systematic errors on the calculated LIC was simulated for various realistic patient measurements with skin–liver distances between 10 and 34 mm, thorax tissue susceptibilities between -9.132 and $-8.532 \cdot 10^{-6} \text{ SI units}$, and LIC between 118 and 12,170 $\mu\text{g Fe/g}_{\text{liver}}$.

Organ Volumes and Analysis of Biomagnetometry Data

The main total body iron stores can be estimated by measuring additionally spleen and liver volumes by sonographic imaging in a similar technique as described by Leung et al. [12]. A 3.5 MHz linear ultrasound probe (length 10 cm) was aligned vertically in its center with a cross-plane laser over the liver or spleen of a patient on the bed of the biosusceptometer. Sagittal (liver) or transversal (spleen) slices at known gap distances were integrated by the imager software (CS100: Picker, Germany). Thus, total body iron stores, U_S , could be calculated from liver (and spleen) iron concentrations, c_{Fe} , as determined by BLS and their organ volumes, V , according to equation 1. Summarizing published results on tissue iron concentration in thalassemia [7], a mean liver (and spleen) total body iron fraction, LIF, of $80 \pm 10\%$ was assumed (see Discussion on this item).

$$U_S = [(c_{\text{Fe}} \cdot V)_{\text{liver}} + (c_{\text{Fe}} \cdot V)_{\text{spleen}}]/\text{LIF}. \quad (1)$$

When performing BLS measurements before t_0 and after t , a certain therapy interval with known iron influx rate from transfusions (K_{in}), the total body iron elimination rate (TBIE) could be calculated according to equation 2. This iron efflux rate may be compared with the usually measured urinary iron excretion rate. Fecal iron excretion rates, otherwise difficult to measure may be calculated by subtraction.

$$\text{TBIE} = K_{\text{in}} + [U_S(t_0) - U_S(t)]/(t - t_0). \quad (2)$$

A two-compartment model for iron balance kinetics in thalassemia was developed along basic ideas of the interaction of transfused and stored iron with chelators [1,13,14] and is outlined in detail in the appendix (Fig. 5). The change of body iron stores due to the particular transfusion and chelation regimen was then interpreted in the framework of this model.

Statistical Methods

Serum ferritin and LIC are well known skewed distributed parameters, especially in iron overload states with a wide range of concentrations. After logarithmic transformation of these parameters a linear correlation can be performed resulting in a meaningful product–moment correlation coefficient r . To characterize group differences, median values and interquartile ranges (50%) were used instead of arithmetic means \pm standard deviations for the same reason. For the calculations and linear regression fits a statistical PC based software package was used (STATISTICA 5.0: StatSoft Inc., Tulsa, OK). The chi-square test was used for fitting the iron balance model, i.e., the elimination rate constants, to the experimental data.

RESULTS

Biomagnetic Liver Susceptometry in Children

All children tolerated the water bag load of 6 to 8 kg very well. Special attention was devoted to the problem of nonliver contributions in the measured SQUID signals because the lung or intestine have magnetic susceptibilities similar to iron loaded tissue. Only low SQUID signals were achieved in the 17 normal children resulting in normal LIC between 60 and 340 $\mu\text{g/g}_{\text{liver}}$ (see Table I). This low range was in agreement with their relatively low serum ferritin levels between 12 and 88 $\mu\text{g/L}$. Moreover, sonographic liver volume estimations in children with thalassemia revealed enlarged organs in the patients by 10 to 140% compared with volume estimations in the group of normal children or as derived from body surface area [15].

Beyond ambient magnetic noise and systematic errors, the precision of the BLS method depends mainly from the reproducibility of the positioning. This could be investigated recently in one patient (Table I: patient RY at an age of 9 years) during initiation of an intensive chelation treatment. BLS measurements started 9 days after beginning of the DFO infusion at a continuous dose of 100 mg/kg/d and were repeated until the 23rd day in intervals of 1 to 4 days. During this period the body weight remained at 35 kg and the mean skin–liver distance from the seven measurements was $15.3 \pm 0.7 \text{ mm}$. The measured LIC values are shown in Figure 1 along the line of the mean value of $5002 \pm 246 \mu\text{g Fe/g}_{\text{liver}}$. The errors of the BLS measurements at the different days were between 214 and 263 $\mu\text{g Fe/g}_{\text{liver}}$, mainly caused by the imprecision in the skin–liver distance.

In half of the nonsplenectomized patients, in whom the spleen volume exceeded 300 ml, biomagnetic spleen iron measurements could be performed (see Table I). Below this limit nonspleen contributions to the SQUID signals were also observed, predominantly from far-field lung

TABLE I. Clinical and Biomagnetometry Data (Median Values and Interquartile Range [–]) of Patients With β -Thalassemia Major, Other Iron Loading Anemias (β -Thalassemia Intermedia, Aplastic Anemia, Congenital Dyserythropoetic Anemia), and Normal Children at First SQUID Measurement. In Addition, Data Are Shown for Individual Patients at the Beginning of Regular Chelation Therapy

Patient groups	n	Age (years)	Serum ferritin ($\mu\text{g/L}$)	Liver iron concentration ($\mu\text{g Fe/g}_{\text{liver}}$)	Spleen iron concentration ($\mu\text{g Fe/g}_{\text{spleen}}$)	Liver volume (ml)	Liver enlargement	Spleen volume (ml)	Total Body storage Fe (g)
β -Thalassemia major	14	10.5 [4–16]	2,847 [1,672–3,629]	3,050 [1,975–5,110]	2,000 [1,450–2,440]	1,016 [880–1,526]	1.6 [1.4–2.0]	293 [252–394]	3.3 [2.4–5.1]
Other anemias	9	15 [9–18]	1,134 [808–1,657]	1,600 [1,002–2,365]	3,200 [1,865–3,460]	1,555 [1,386–2,034]	1.7 [1.4–1.8]	559 [505–573]	4.7 [2.2–6.9]
Normal subjects	16	12.5 [10–15]	27.5 [16–39]	170 [110–218]	n.d.	1,013 [825–1,467]	0.97 [0.94–1.04]	n.d.	0.28 [0.22–0.34]
Patient									
OP	1	6.3	5,963	8,150	2,880	954	2.07	318	10.94
PP	1	4.6	3,882	6,880	1,990	980	1.76	214	8.96
RY	1	4.5	3,629	4,388	2,390	980	2.33	155	5.84
MB	1	3.5	1,391	2,881	1,540	841	1.94	300	3.61
YD	1	3.1	2,378	3,093	1,500	760	2.91	200	3.46

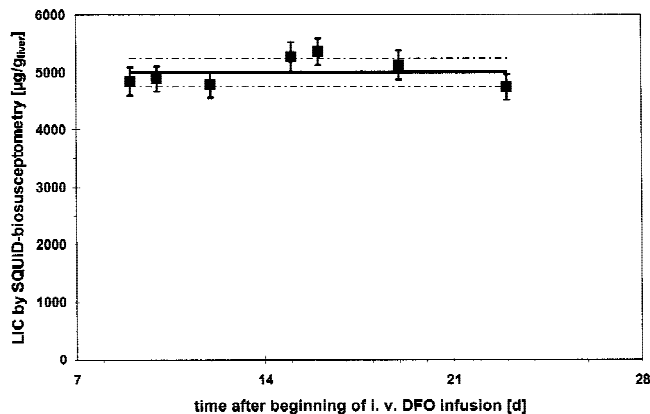


Fig. 1. Short-term reproducibility of LIC assessment by SQUID biomagnetometry during intensive i.v. chelation treatment with DFO in a child (9 years, 35 kg, 132 cm) with β -thalassemia major. Mean LIC value (solid line) \pm 1 standard deviation (dot-dashed lines).

contributions, and the net signal was corrected by a small error term [10]. This procedure could not be applied to the smaller sized spleens covered at half by the lungs in the normal subjects.

In Vivo LIC and Serum Ferritin

LIC obtained from biomagnetic measurements in patients and normal subjects ranged from 580–11,170 and 60–340 $\mu\text{g/g}_{\text{liver}}$, respectively. Spleen iron concentrations were measured in seven patients and varied between 530 and 3,720 $\mu\text{g/g}_{\text{spleen}}$. With the knowledge of the actual liver and spleen volumes by sonographic scanning and the organ iron concentrations, an estimation of the total body iron stores was made on the basis that liver (and spleen) iron account for 80% of total body iron (see equation 1).

The serum ferritin concentration, a parameter widely used in monitoring iron overload in patients with iron loading anemias, especially under chelation therapy, correlates significantly with LIC ($r = 0.64$, $P < 10^{-3}$; dot-dashed line in Figure 2), but is a very poor guide to the iron overload status of an individual, or to the efficacy of the iron chelation therapy (Fig. 3). Linear correlation coefficients could be calculated only after logarithmic transformation of serum ferritin and LIC due to the skewed distribution (skewness = 1.4 and 2.4, respectively). A better correlation with iron load was found for liver volumes ($r = 0.75$, $P < 10^{-3}$). The liver volumes were found to increase by 18% per 1,000 $\mu\text{g/g}$ within the range from 600 to 11,000 $\mu\text{g/g}_{\text{liver}}$.

For the purpose of a quantitative estimation of LIC from serum ferritin an a priori linear function was fitted to all data including normals (Fig. 2: solid line, $r^2 = 0.78$). Additionally, the 95% prediction lines are shown in Figure 2 resulting in a prediction interval for thalassemic patients from 30 to 3,970 $\mu\text{g/g}_{\text{liver}}$ at their median value of 3,050 $\mu\text{g/g}_{\text{liver}}$.

Model Derived Biomagnetometry Data

The compartment model, developed for iron balance kinetics in thalassemia and as outlined in the appendix in more detail, was applied to the data of a patient with β -thalassemia major (Table I, patient OP: m, 6.3 years, 20 kg at 1st SQUID measurement). Total body iron stores were calculated from liver and spleen iron concentration and the respective volumes according to equation 1. The analysis of the biomagnetically measured total body iron stores (squares) in the framework of this model is displayed in Figure 3.

The hypothetical iron accumulation before the beginning of chelation treatment and the decrease of iron

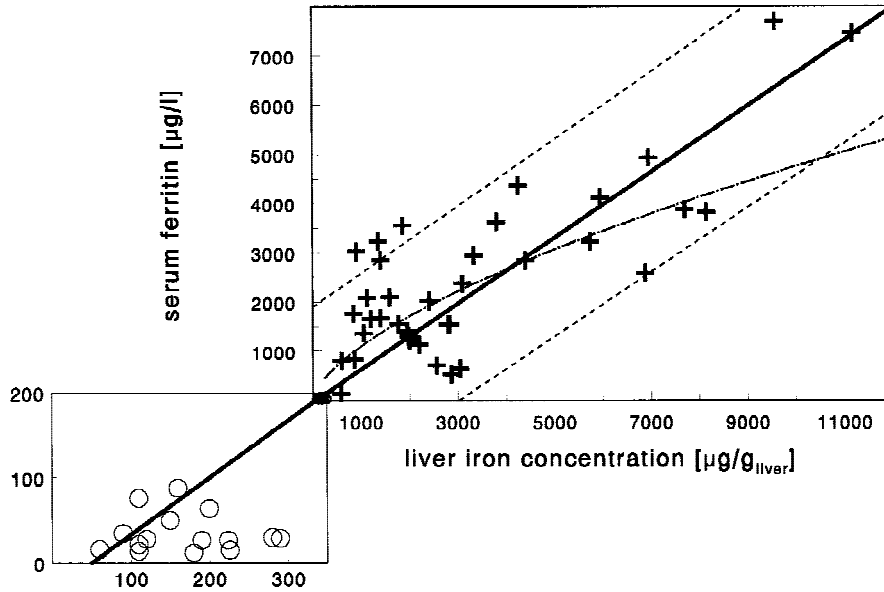


Fig. 2. Correlation after logarithmic transformation between LIC assessed by SQUID biomagnetometry vs. serum ferritin in children with transfusion siderosis (+, $r = 0.64$, dotted-dashed line). Linear regression analysis ($r^2 = 0.78$, solid line) with 95% prediction range (dashed lines) for all subjects including normal children (O).

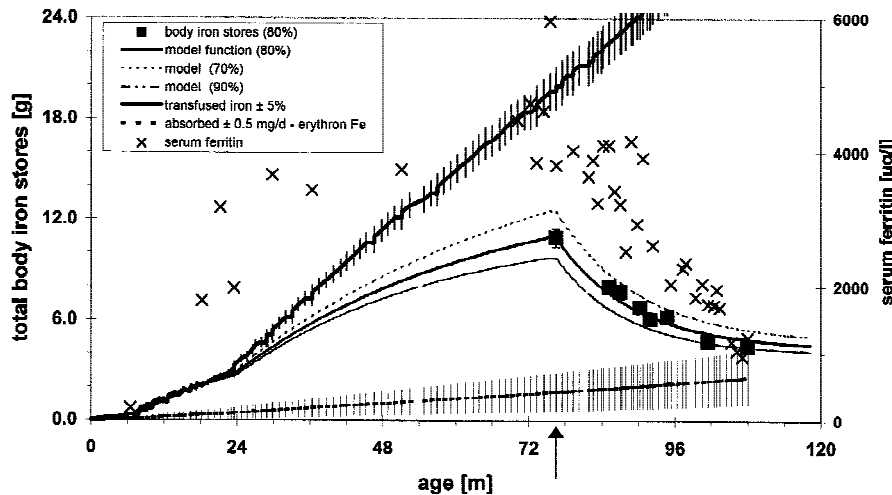


Fig. 3. Accumulation of iron caused by regular transfusion therapy (mean rate = 10.6 ± 0.5 mg Fe/d, upper hatched band) and absorbed iron (1.0 ± 0.5 mg/d, lower hatched band): total body iron stores estimated from liver and spleen iron ($\approx 80\%$) before and during chelation therapy with DFO (onset marked by arrow) and L1 in patient OP since time of birth.

stores due to regular and alternating DFO/L1-chelation therapy is shown over 9 years since birth (solid line). The effective net iron influx K_{in} was calculated mainly from the transfusion rate ($K_T = 10.6$ mg iron/d). Additionally, the absorbed iron from nutrition at a mean rate of $K_N = 1.0 \pm 0.5$ mg Fe/d was taken into account reduced by the iron needs of the growing blood volume dU_B/dt (see hatched bands in Figure 3). Thus, the net iron influx was given by $K_{in} = 11.40 \pm 0.54$ mg/d. The influence of different liver-spleen storage iron fractions ($LIF = 80 \pm 10\%$) on the total body iron stores and therefore on the iron accumulation curve is also shown in Figure 3 (dotted and dotted-dashed lines). The model curve function before regular chelation treatment was adjusted to the 1st SQUID measurement by a basal iron elimination rate constant $k_{e1} = 0.08 \pm 0.02$ %/d. The exponential part was fitted to the experimentally determined body iron

stores by an increased elimination rate constant $k_{e1} = 0.265 \pm 0.020$ %/d during the chelation treatment with alternating rates of DFO ($K_{ch} = 85$ mg/kg/d) and L1 ($K_{ch} = 70$ mg/kg/d).

A further result within this model was the forecasting of the maximum therapy effect (extrapolated solid curve in Figure 3) until steady-state conditions will be achieved at a total body iron store of $U_S(t \rightarrow \infty) = 4.3$ g. Moreover, no significant difference in the elimination rate constants could be derived from the DFO and L1 therapy intervals from this patient in Figure 3 [8]. This may become different after the equilibrium between transfused and chelated iron is reached. The wider scatter of serum ferritin data, which are normally used for monitoring, provided only a broad guide to the biomagnetically determined iron stores.

In five thalassemic children BLS could be performed

TABLE II. Elimination Rate Constants Derived From Model Fit to the Experimental Data Before (k_{el}^o) and After the Start (k_{el}) of Regular Chelation Therapy by s.c. DFO: Resulting TBIE Rates Depend on the Actual Size of Iron Stores*

Patients	Final total body storage Fe (g)	K_T transfusion rate (mg/d)	K_{in} Fe influx rate (mg/d)	K_{ch} chelation rate (mg/kg/d)	C_{ch} specific chelation rate (mmol/d/g Fe)	k_{el}^o basal elimination const. (%/d)	k_{el} elimination rate constant (%/d) ^a	TBIE initial rate (mg/d)
OP	4.43	10.6	11.4	63	0.198	0.08	0.27	27
PP	3.15	11.9	12.6	80	0.348	0.03	0.38	31
RY	5.95	9.2	9.8	11	0.070	0.13	0.16	9
MB	—	4.9	5.6	—	—	0.06	—	—
YD	1.29	7.5	8.3	89	0.689	0.06	0.83	23

*TBIE, total body iron elimination.

^aLinear regression fit: $k_{el} = 0.05 + 1.10 \cdot C_{ch}$ ($r^2 = 0.98$, see equation 5 of appendix).

before starting regular chelation therapy with s.c. DFO. As already demonstrated in Figure 3, the accumulated total influx of iron exceeded the measured total iron store by far. This discrepancy could be overcome by assuming a basal iron elimination from 0.03 (normal) to 0.13 %/d. The data for the elimination rate constants k_{el} in Table II could be fitted by a linear function of the ratio between the chelation rate K_{ch} (Table II) and the initial iron store (Table I), i.e., the specific chelator concentration C_{ch} (see approximation of equation 5 in the appendix). The relation between the elimination rate constant and the specific chelator concentration should reflect to some extent the therapy efficacy of a chelator under investigation and/or the patient's compliance. From the data in Table II a linear regression coefficient of 1.10 ± 0.09 (%/d)/(mmol/d/gFe) was calculated ($r^2 = 0.98$), with an intercept at 0.05 ± 0.04 %/d indicating the mean basal elimination rate constant of these five patients.

DISCUSSION

Biomagnetic Liver Susceptometry in Children and Young Adults

The low SQUID signals with resulting normal LIC achieved in the 17 normal children, demonstrate that the spatial resolution of the biosusceptometer detector and field coil configuration was adequate, allowing nonliver contributions in the measured signals of the relatively small-sized patients to be ignored. In children with normal LIC, the body tissue susceptibility is the parameter with the strongest effect on the resulting iron concentration. However, in many of the relatively young and slim patients with thalassemia, this patient background is less important. Moreover, the enlarged organs in these patients allow easy positioning, and especially, also the measurement of spleens (>300 ml) in almost all patients. As BLS is measuring magnetic susceptibilities from ferritin and hemosiderin iron, there is no principle difference between the in vivo determination of iron in liver or spleen. Nevertheless, biomagnetical and biochemical determinations of spleen iron concentrations should be es-

tablished in the future in order to rule out any possible perturbations from lungs, intestine, or blood flow.

The impact of various error contributions from geometry parameters (liver and thorax), skin–liver distance ($\Delta z = \pm 0.5$ mm), or magnetic thorax susceptibility of the overlying tissue ($\Delta\chi = \pm 0.05 \cdot 10^{-6}$ SI units) on the LIC has been studied by variation of these parameters in realistic patient measurements [16]. Exemplarily, this procedure results in a total error of 98 $\mu\text{g Fe/g}_{liver}$ for a patient with an LIC of 563 $\mu\text{g Fe/g}_{liver}$, but of 286 $\mu\text{g Fe/g}_{liver}$ for another patient with an LIC of 6,414 $\mu\text{g Fe/g}_{liver}$. In comparison, variation of liver and thorax geometry (unless in very small-sized organs) had only a marginal effect on the LIC. For LIC above 5,000 $\mu\text{g Fe/g}_{liver}$, the precision in the liver depth ($\Delta z \geq 0.3$ mm) is the major determinant of the total error (3.5%) of the calculated iron concentration. Thus, the overall error in realistic measurements of children and young adults is between 50 and 300 $\mu\text{g/g}_{liver}$, depending mainly on the skin–liver distance and the fat contribution in the overlying thorax tissue (ribs, muscle, fat) of the liver. This is due to the poor spatial resolution in current biosusceptometer sensor designs with resulting inaccurate estimation of magnetic susceptibilities of the thorax tissue [10].

A similar correlation of serum ferritin with LIC determined by biomagnetic liver susceptometry was found by Brittenham et al. [17] in 111 patients with thalassemia major and sickle cell anemia with LIC between 283 and 15,987 $\mu\text{g/g}_{liver}$. The patients in this previous study were, however, of greater mean age (19 years). From linear regression analysis, an even poorer coefficient of determination of $r^2 = 57\%$ was found for serum ferritin. The smaller variability of serum ferritin in this study was caused in part by the inclusion of normal subjects, which fixed the intercept of the regression line. Estimating a liver iron concentration of 3,000 $\mu\text{g/g}_{liver}$ from the corresponding serum ferritin determination was only possible within a 95% prediction interval of 8,000 $\mu\text{g/g}_{liver}$ [17], which is certainly inadequate for adjusting chelation therapy to body iron stores as the prediction interval of 4,000 $\mu\text{g/g}_{liver}$ in this study. The variability of serum

ferritin in iron overload states has been attributed to ongoing inflammation processes and cell damage [18,19]. However, serum ferritin values in the presence of elevated ALT levels have been largely excluded and only few patients were positive for HCV infection in our group of patients. The iron regulatory proteins (IRP-1 and IRP-2) as cytoplasmic sensors of the labile iron pool, control the ferritin synthesis by iron-dependent reciprocal binding to iron responsive elements (IRE) of mRNAs for the H and L subunits of ferritin [20]. However, also iron-independent modulation of IRP activity takes place by oxidative stress, nitric oxide production, hyperthyroidism, and inflammatory cytokines [21]. Moreover, distinct differences between serum and tissue ferritin and probably different encoding genes [22] may explain the observed serum ferritin variability in assessing the human iron status.

Total Body Iron Stores

Non-heme total body iron stores in thalassemia and the resulting liver (and spleen) iron fraction have been estimated from the physico-chemical determination of iron in various tissues of thalassemic patients mostly at post-mortem or from comparison of total liver iron with the accumulated iron from transfusion [7]. From the data of Barry et al. [23], Modell and Berdoukas found an agreement within $\pm 15\%$ between transfused iron and the amount recovered in the liver at postmortem [7, p 168]. Summing-up the measurements of tissue iron concentration so far published in the literature and combining these with the respective tissue masses normalized to 50 kg according to ICRP 23 [24]^a then liver and spleen storage iron fractions of 70 to 85% of the total sum are achieved with a likely tendency to higher values in patients treated with current therapy. Selected typical minimum and maximum tissue iron concentrations have been calculated as $\text{mg/g}_{\text{wet weight}}$ with a drying factor of 5 [7] or 3.5 [other references] for dry weight iron concentrations. The relative amounts as calculated from the total sum are given in brackets {}: liver [7] 7.4–13.6 {79–69%}, muscle [7] 0.12–0.28 {13–14%}, spleen [7,25] 1.4–5.4 {4–7%}, heart wall [7,26] 1.2–2.6 {1.5%}, red marrow [7,27] 0.02–202 {0.1–5.5%}, and pancreas [7] 2.8–7.8 {1.1–1.4%}. The contribution of other tissues and organs to the total iron store seems to be negligible as from glands [7] {1%}, kidney (1%), skin [28] {0.2–0.7%}, and lung (?). Liver storage iron fractions between 70 and 90% were received from comparison of mobilized iron by phlebotomy therapy in genetic hemochromatosis with liver iron quantitation by biopsies [29] and by BLS (data not published). Thus, a value of LIF = 80% for the mean

liver storage iron fraction may be assumed as a reasonable value in the model calculations.

Iron Balance Kinetics (Analysis of Biomagnetometry Data)

The exponential character of the chelator–(storage) iron interaction, although not defined in a mathematical formulation, has been noticed by many authors in the past [23]. It can be derived already from the conclusions in the work of Modell and of Brittenham based on two different phenomena:

1. the steady fall of urinary iron excretion in long-term desferrioxamine therapy [13]; a fixed dose of desferrioxamine produces progressively less iron excretion as the liver iron concentration falls [14];
2. the equilibrium between transfused iron and spontaneous or chelation-induced iron excretion reached at appreciable body iron burdens [1,14,23].

Thus, patients under a constant transfusion and chelation therapy regimen will reach 90% of their equilibrium total iron burden after 1–3 years with elimination rate constants between 0.6 to 0.2 %/d, respectively.

Iron absorption in thalassemia for patients under current high transfusion regimens is not well investigated due to the inherent difficulties of labeling and standardizing human food. Most studies in the past have used extrinsically ^{59}Fe -labeled heme iron [30], non-heme iron [31,32], or both [33] adjusted to 5 mg doses. Absorption from intrinsically ^{59}Fe -labeled food iron (pork) has been determined only in one patient with thalassemia major [34]. There is a broad agreement in the inverse relationship between iron absorption and hemoglobin level. Transfusion regimens maintaining minimum hemoglobin levels of 9 g/dl will give rise to an iron absorption of about 10% from a 5 mg dose [31,33]. This seems to be comparable with iron absorption values observed in subjects with normal iron stores [30,34]. Thus, the assumption of an average iron absorption rate of 1 mg/d from a mixed diet seems reasonable, especially taking into account phyto-inhibitors for iron absorption. Additionally, there is evidence that subcutaneous DFO infusions reduce absorption of inorganic iron [31]. This may further reduce larger values given by other authors [34,35]. In comparison to the averaged transfused iron of 12 mg/d (Table II) this nutritional iron seems to have only a small influence on the model-derived elimination rate constant. During growth, moreover, part of this iron influx is counterbalanced by the iron needs for the increasing blood volume [36]. However, applying the model to patients with thalassemia intermedia will give rise to a larger influence of iron absorption rates upon model derived parameters.

Iron elimination in thalassemia is mainly derived from urinary iron excretion studies. Iron balance studies with

^aFor liver and spleen in thalassemic patients, typical volumes of 2,000 and 500 ml have been assumed, respectively.

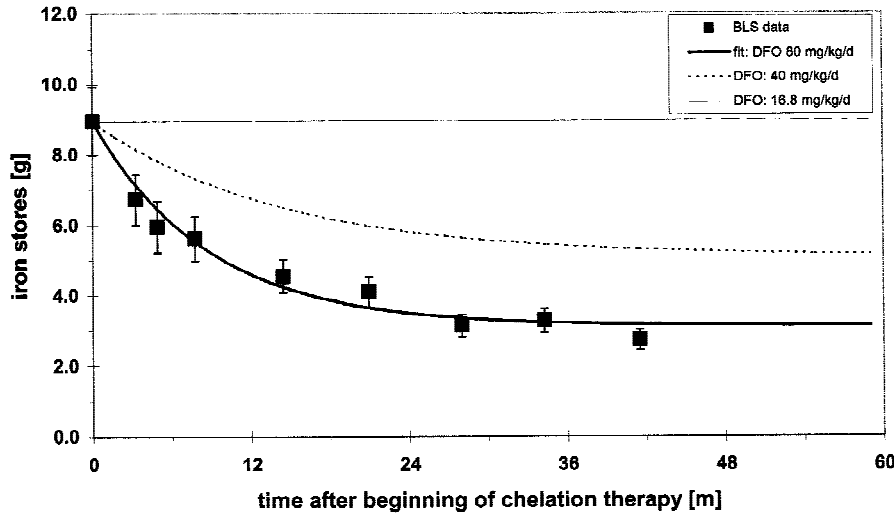


Fig. 4. Response from different therapy regimens extrapolated from the compartment model for iron balance kinetics in thalassemia compared with the outcome in patient PP.

the additional determination of iron in the feces are difficult to perform in the presence of a high background of food iron. There are very few studies exploiting the possibility of labeling the iron stores with ^{59}Fe . Elimination rate constants between 0.02 and 0.088 %/d for iron loss were found in normal males and iron loaded Bantu subjects with non-heme iron stores between 0.3 and 4.0 g, respectively [37]. Mean basal (^{59}Fe) iron excretion rate constants of 0.04 and 0.038 %/d were observed in the urine and feces of transfused thalassemic patients [38]. Modell and Beck [13] reported up to five times higher amounts of iron loss when comparing mean urinary iron excretion values from normal patients with those from transfused thalassemic patients. Higher urinary iron losses were also found in iron overloaded ex-thalassemic patients after bone marrow transplantation [39]. Therefore, larger basal iron elimination rate constants for thalassemic patients as found in Table II seem to be reasonable, although part of this increase is caused by sporadically given amounts of DFO together with the transfusion.

Urinary iron excretion values between 5 and 90 mg/d have been measured in various studies in the past [40–45] at comparable s.c. DFO chelation regimens of about 15–70 mg/kg/d. For estimation of total body elimination rates one has also to take into account an additional portion of 25–45% from fecal iron excretion [44] and the corresponding total body iron load. A saturation effect has been reported for s.c. DFO doses beyond 2 g/d or 3.5 mmol/d [41–43]. However, fecal excretion seems to increase linearly for DFO doses in this range [44]. These data are in agreement with those of Table II and with the conceptions of the model in the appendix. The saturation effect will be less pronounced for DFO, especially, at lower specific chelator concentrations, i.e., larger iron stores. Thus, the approximation of a linear relationship

between the efficacy of DFO and the specific chelator concentration (see appendix, equation 5) seems to be reasonable and can also be concluded from the linear regression fit in Table II. Actual total body iron elimination rates can be calculated from the iron stores and the transfusion rate (see equations 4 and 2). TBIE rates have been calculated in Table II for the initial iron stores at the beginning of chelation treatment in the four selected patients. Final TBIE rates will converge to the iron influx rates when steady-state conditions are achieved as in patient PP.

Analyzing iron stores by model simulations could be helpful in deriving the individual chelator therapy efficacy. In Figure 4 this is demonstrated by a perfect fit through the experimental data of the patient PP. This was achieved by a constant elimination rate constant of 0.382 ± 0.036 %/d. After 48 months the asymptotic value of $K_{\text{in}}/k_{\text{e1}} = 12.6/0.00382 = 3.3$ g Fe is achieved (see Table II and appendix). This corresponds with a biologically determined LIC of $1,540 \mu\text{g/g}_{\text{liver}}$, which was certified two months later in a liver biopsy at $1,520 \mu\text{g/g}_{\text{wet weight}}$. Iron stores will not decrease further as long as no improvement in the chelation therapy regimen is made. Assuming a linear response to the specific chelator concentration C_{ch} as could be derived from the data in Table II and from equation 5 in the appendix, elimination rate constants were calculated for different chelation rates. At 16.8 mg/kg/d total body iron excretion would be in equilibrium with the iron influx from transfusions. For a more exact solution of this problem, a nonlinear approach for the iron elimination in response to a specific chelator concentration has to be assumed. Especially at lower iron concentrations corresponding with larger specific chelator concentrations saturation effects have to be expected for certain chelators (e.g., L1).

CONCLUSIONS

Noninvasive magnetic biopsy may become the method of choice to determine liver and spleen iron content in iron overloaded patients. Especially in thalassemic children iron stores change relatively fast due to a frequent adjustment of therapy and have to be monitored regularly. Magnetic contributions from the lung or intestine to the measured SQUID liver signals in the small-sized patients were not observed. Further efforts have to be undertaken for a reliable measurement of spleen iron by biomagnetometry also for smaller volumes. Serum ferritin values do allow the prediction of LIC only with a precision of 4,000 to 8,000 $\mu\text{g/g}_{\text{liver}}$. With the simultaneous determination of the actual organ volumes we were able to estimate directly the total body iron stores probably within $\pm 10\%$.

A simple compartment model for the quantitative description of the iron balance kinetics in thalassemia was developed. Analyzing the experimental data from biomagnetometry within the framework of this model, we were able to derive information on total body iron elimination, chelation effectiveness, which is directly related to compliance, and on forecasting steady-state conditions of iron load with a particular chelation therapy regimen. For the first time an approach has been made to formulate the interaction of a chelator with the iron stores and the transfusion rate in a quantitative way. More patient measurements under a well-defined therapy regimen will be needed for a reliable quantitative formulation of the dose response of chelators.

The determination of the main iron stores in liver and spleen tissues by noninvasive biomagnetic susceptometry offers an important diagnostic technique for the optimization of iron chelation therapy with subcutaneous DFO infusions and for the control of the efficacy of newly developed oral chelators (e.g., L1/CP20). Long-term monitoring of the LIC, the parameter most closely related to iron overload, may also act as a spur to increased compliance with chelation therapy.

ACKNOWLEDGMENTS

We are indebted to Martin J. Pippard for critically reviewing this paper and gratefully acknowledge his contributions to the discussion.

REFERENCES

- Modell CB. Transfusional haemochromatosis. In: Kief H, editor. Iron metabolism and its disorders. Amsterdam: Excerpta; 1975. p 230–240.
- Brittenham GM. Noninvasive methods for the early detection of hereditary hemochromatosis. *Ann NY Acad Sci* 1988;526:199–208.
- Brittenham GM, Farrell DE, Harris JW, Feldman ES, Danish EH, Muir WA, Tripp JH, Bellon EM. Magnetic susceptibility measurement of human iron stores. *N Engl J Med* 1982;307:1671–1675.
- Fischer R, Engelhardt R, Nielsen P, Gabbe EE, Heinrich HC, Schmieg WH, Wurbs D. Liver iron quantification in the diagnosis and therapy control of iron overload patients. In: Hoke M, Ern  SN, Okada YC, Romani GL, editors. Biomagnetism: clinical aspects. Amsterdam: Elsevier; 1992. p 585–588.
- Fischer R, Piga A, Tricta F, Nielsen P, Engelhardt R, Garofalo F, Di Palma A, Vullo C. The use of biomagnetic liver susceptometry in the Ferrara-Hamburg-Turin study on thalassemia. In: Aine CJ, Okada YC, Stroink G, Swithenby SJ, Wood C, editors. BIOMAG96: Advances in Biomagnetism Research. New York: Springer; 1998. (in press).
- Hartmann W, Schneider L, Wirth A, D rdelmann M, Zinser D, Elias H, Languth W, Ludwig W, Kleihauer E. Liver susceptometry for the follow up of transfusional iron overload. In: Hoke M, Ern  SN, Okada YC, Romani GL, editors. Biomagnetism: clinical aspects. Amsterdam: Elsevier; 1992. p 589–593.
- Modell B, Berdoukas V. The clinical approach to thalassemia. London: Grune & Stratton; 1984. p 163–169, 215.
- Nielsen P, Fischer R, Engelhardt R, Tond ry P, Gabbe EE, Janka GE. Liver iron stores in patients with secondary haemochromatosis under iron chelation therapy with deferoxamine or deferiprone. *Br J Haematol* 1995;91:827–833.
- Paulson DN, Fagaly RL, Toussaint RM, Fischer R. Biomagnetic susceptometer with SQUID instrumentation. *Inst Electr Electron Eng Trans Magn* 1991;27:3249–3252.
- Fischer R. Liver iron susceptometry. In: Andrae W, Nowak H, editors. Magnetism in medicine: a handbook. Berlin: Wiley-VCH; 1998. p 286–301.
- Shoden A, Sturgeon P. Hemosiderin—a physico-chemical study. *Acta Haematol* 1960;23:376–392.
- Leung NWY, Farrant P, Peters TJ. Liver volume measurement by ultrasonography in normal subjects and alcoholic patients. *J Hepatol* 1986;2:157–164.
- Modell CB, Beck J. Long-term desferrioxamine therapy in thalassemia. *Ann NY Acad Sci* 1974;232:201–210.
- Brittenham GM, Allen CJ, Farrell DE, Harris JW. Hepatic iron stores in thalassemia: non-invasive magnetic measurements. *Prog Clin Biol Res* 1989;309:101–106.
- Rasmussen N. Liver volume determination by ultrasonic scanning. *Dan Med Bull* 1978;25:1–45.
- Tiemann C. Biomagnetometrische Speichereisen-Bestimmung: Therapiekontrolle bei Kindern mit Transfusions siderosen [Thesis]. University Hamburg; 1995. p 28–30.
- Brittenham GN, Cohen AR, McLaren CE, Martin MB, Griffith PM, Nienhus AW, Young NS, Allen CJ, Farrell DE, Harris JW. Hepatic iron stores and plasma ferritin concentration in patients with sickle cell anemia and thalassemia major. *Am J Hematol* 1993;42:81–85.
- De Virgili S, Sanna G, Cornacchia G, Argioli F, Murgia V, Porcu M, Cao. Serum ferritin, liver iron stores, and liver histology in children with thalassemia. *Arch Dis Child* 1980;55:43–45.
- Worwood M, Cragg SJ, Jacobs A, McLaren C, Ricketts C, Economidou J. Binding of serum ferritin to concanavalin A: patients with homozygous β thalassemia and transfusional iron. *Br J Haematol* 1980;46:409–416.
- Hentze MW, Kuehn LC. Molecular control of vertebrate iron metabolism: mRNA-based regulatory circuits operated by iron, nitric oxide, and oxidative stress. *Proc Natl Acad Sci USA* 1996;93:8175–8182.
- Ponka P, Beaumont C, Richardson. Function and regulation of transferrin and ferritin. *Blood* 1998;35:35–54.
- Linder MC, Schaffer KJ, Hazegh-Azam M, Zhou CY, Tran TN, Nagel GM. Serum ferritin: does it differ from tissue ferritin? *J Gastroenterol Hepatol* 1996;11:1033–1036.
- Barry M, Flynn DM, Letsky EA, Risdon RA. Long-term chelation

- therapy in thalassemia major: effect on liver iron concentration, liver histology, and clinical progress. *Br Med J* 1974;2:16–20.
24. ICRP Publication 23. Reference man: anatomical, physiological and metabolic characteristics. Oxford: Pergamon; 1975, table 105.
 25. Cazzola M, Borgna-Pignatti C, De Stefano P, Bergamaschi G, Bongo IG, Dezza L, Avato F. Internal distribution of excess iron and sources of serum ferritin in patients with thalassemia. *Scand J Haematol* 1983;30:289–296.
 26. Buja LM, Roberts WC. Iron in the heart. *Am J Med* 1971;51:209–220.
 27. Bezuda WR, Bothwell TH, Torrance JD, MacPhail AP, Charlton RW, Kay G, Levin J. The relationship between marrow iron stores and plasma ferritin concentrations and iron absorption. *Scand J Haematol* 1979;22:113–120.
 28. Gorodetski R, Loewenthal E, Goldfarb A, Rachmilewitz EA. Non-invasive evaluation of iron load and clearance in patients with β -thalassemia. *Ann NY Acad Sci* 1990;612:568–572.
 29. Summers KM, Halliday JW, Powell LW. Identification of homozygous hemochromatosis subjects by measurement of hepatic iron index. *Hepatology* 1990;12:20–25.
 30. Bannerman RM, Callender ST, Hardisty RM, Smith RS. Iron absorption in thalassemia. *Br J Haematol* 1964;10:490–495.
 31. Pippard MJ, Callender ST, Warner GT, Weatherall DJ. Iron absorption in iron-loading anaemias: effect of subcutaneous desferrioxamine infusions. *Lancet* 1977;i:737–739.
 32. Pootrakul P, Kitcharoen K, Yansukon P, Wasi P, Fucharoen S, Charoenlarp P, Brittenham G, Pippard MJ, Finch CA. The effect of erythroid hyperplasia on iron balance. *Blood* 1988;71:1124–1129.
 33. Alarcon PA, Donovan ME, Forbes GB, Landaw SA, Stockman JA. Iron absorption in the thalassemia syndromes and its inhibition by tea. *N Engl J Med* 1979;300:5–8.
 34. Heinrich HC, Gabbe EE, Oppitz KH, Whang DH, Bender-Götze C, Schäfer KH, Schröter W, Pfau AA. Absorption of inorganic and food iron in children with heterozygous and homozygous β -thalassemia. *Z Kinderheilk* 1973;115:1–22.
 35. Erlandson ME, Walden B, Ster G, Hilgartner MW, Wehman J, Smith CH. Studies on congenital hemolytic syndromes: IV. Gastrointestinal absorption of iron. *Blood* 1962;19:359–378.
 36. Gabutti V, Piga A, Fortina P, Miniero R, Nicola P. Correlation between transfusion requirement, blood volume and haemoglobin level in homozygous β -thalassemia. *Acta Haematol* 1980;64:103–108.
 37. Green R, Charlton R, Seftel H, Bothwell T, Mayet F, Adams B, Finch C, Layrisse M. Body iron excretion in man. *Am J Med* 1968;45:336–353.
 38. Malamos B, Constantoulakis M, Gyftaki E, Kesse-Elias M, Augoustaki O. Urinary and faecal iron excretion in thalassemia syndromes. *Acta Haematol* 1969;42:321–329.
 39. Politi P, Lucarelli G, Capriotti L, Salvadori P, Pardanelli C, Barbanti I. Liver iron stores before and after bone marrow transplantation for thalassemia. *Prog Clin Biol Res* 1989;309:281–289.
 40. Propper RD, Cooper B, Rufo RR, Nienhuis AW, French Anderson W, Franklin Bunn H, Rosenthal A, Nathan DG. Continuous subcutaneous administration of desferrioxamine in patients with iron overload. *N Engl J Med* 1977;297:418–423.
 41. Pippard MJ, Callender ST, Weatherall DJ. Intensive iron-chelation therapy with desferrioxamine in iron-loading anaemias. *Clin Sci Mol Med* 1978;54:99–106.
 42. Pippard MJ, Callender ST, Letsky EA, Weatherall DJ. Prevention of iron loading in transfusion-dependent thalassemia. *Lancet* 1978;i:1178–1181.
 43. Janka GE, Möhring P, Helmig M, Haas RJ, Betke K. Intravenous and subcutaneous desferrioxamine therapy in children with severe iron overload. *Eur J Pediatr* 1981;137:285–290.
 44. Pippard MJ, Callender ST, Finch CA. Ferrioxamine excretion in iron loaded man. *Blood* 1982;60:288–294.
 45. Fargion S, Taddei MT, Gabutti V, Piga A, Di Palma A, Capra L, Fontanelli G, Avanzini A. Early iron overload in beta-thalassemia

major: when to start chelation therapy? *Arch Dis Childhood* 1982;57:929–933.

APPENDIX

Compartment Model for Iron Balance Kinetics in Thalassemia

This dynamic model (see Figure 5) is based on the balance between iron influx rate (predominantly transfused iron) and iron elimination induced change of total body iron stores (see equation 3 of appendix). It depends also on the assumed ratio between liver (+spleen) iron and total body iron stores, the so-called liver (+spleen) storage iron fraction LIF (see equation 1).

The iron transfusion rate K_T [mg Fe/d] and, in well transfused thalassemic patients, to a minor degree, the iron absorption rate K_N , transfer iron via the blood pool $U_B(t)$ into the body iron store $U_S(t)$. Especially during growth one also has to take into account an increasing blood iron pool that will compensate part of the total iron influx rate, i.e., $dU_B/dt < 0$. The chelation efficacy of any chelator (desferrioxamine, DFO or deferiprone, L1) shows up as the iron elimination rate constant k_{el} [d^{-1}]. The initial total body iron store at the beginning of treatment with a chelator rate K_{ch} is defined by $U_S(t_0)$. In a good

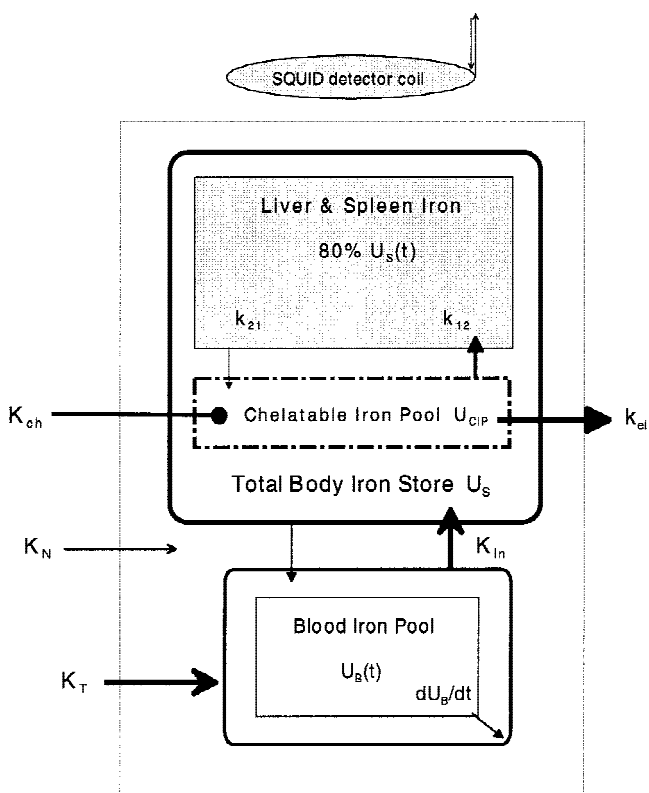


Fig. 5. Compartment model for iron balance kinetics in iron loading anaemias. Assessment of 80% of total body iron stores by SQUID biomagnetic liver (and spleen) susceptometry.

approximation (assuming the chelatable iron pool U_{CIP} is a small transition pool in equilibrium with the storage pool, i.e., $dU_{CIP}/dt = 0$), the total body iron store can be described by a linear 1st order differential equation, with the total influx rate $K_{in} = K_T + K_N - dU_B/dt$, and with $k_{e1} = \text{constant}$.

$$dU_S/dt = K_{in} - k_{e1}(K_{ch}, U_{CIP}) \cdot U_S \quad (3)$$

Under steady-state conditions, i.e., $dU_S/dt = 0$, the elimination rate constant can be easily determined from a single BLS measurement and the known transfusion rate. In 1st order approximation, one can take into account only the influx from transfused iron. This differential equation is solved analytically by the function 4 assuming a constant iron influx over the time interval $\Delta t = t - t_o$.

$$U_S(t) = K_{in}/k_{e1} \cdot [1 - \exp(-k_{e1} \cdot \Delta t)] + U_S(t_o) \cdot \exp(-k_{e1} \cdot \Delta t). \quad (4)$$

A least square fit of this function to the experimental data (body iron stores $U_S(t)$, and total iron influx rate K_{in}) results in the determination of total iron elimination rate

constants k_{e1} . The integral $\int k_{e1} \cdot U_S(t) dt$ over a certain therapy interval $\Delta t = t - t_o$ results in the model independent total body iron elimination TBIE as mentioned earlier in equation 2. The iron balance rate $TBIE - K_{in} = [U_S(t_o) - U_S(t)]/\Delta t$, depends mainly on possible changes in the transfusion regimen during the time of observation.

In 2nd order, the elimination rate constant K_{e1} will depend also on the concentration of the chelator dosage K_{ch} and the non-heme iron within the chelatable iron pool $U_{CIP}(t)$, which is assumed to be proportional to the iron store U_S itself. In good approximation (at least for DFO), one could assume a linear relationship as in equation 5 with the specific chelator concentration $C_{ch} = K_{ch}/U_S$ and the basal elimination rate constant $k_{e1}^o \approx 0.06 \text{ \%}/d$.

$$k_{e1} = k_{e1}^o + \text{const} \cdot C_{ch}. \quad (5)$$

In this approximation, the elimination rate constant k_{e1} will depend inversely on the actual storage iron pool $U_S(t)$, will also be adjusted for possible changes in the chelation regimen, will be independent of the transfusion rate, and will characterize the combined effect from therapy efficacy and patient compliance.